IEEE Access
Multidisciplinary | Rapid Review | Open Access Journal

SPECIAL SECTION ON EMERGING DEEP LEARNING THEORIES AND METHODS FOR BIOMEDICAL ENGINEERING

Received May 12, 2020, accepted May 23, 2020, date of publication June 10, 2020, date of current version July 20, 2020.

Digital Object Identifier 10.1109/ACCESS.2020.3001212

Application of Deep Learning Algorithm in Clinical Analysis of Patients With Serum Electrolyte Disturbance

JIAN WANG*, YAN PING WANG*, YAO CHEN, AND PEIJI HUANG

Department of Endocrinology and Metabolism, Fujian Institute of Endocrinology, Fujian Medical University Union Hospital, Fuzhou 350001, China

Corresponding author: Jian Wang (wj_fjfz@163.com)

*Jian Wang and Yan Ping Wang are co-first authors.

ABSTRACT This article analyzes the serum electrolyte disturbances of patients through deep learning algorithms. Among the 104 patients with electrolyte disturbances, 6 cases of serum potassium, sodium, chloride, calcium, phosphorus, and magnesium electrolyte disturbances have occurred, the proportion of occurrence The order is sodium > chlorine > calcium > potassium > phosphorus > magnesium. This paper proposes a deep learning algorithm for serum electrolyte disorder, and analyzes and implements the functions at various levels according to the characteristics of the Hadoop framework. The system includes electronic medical records shared storage, distributed realization of definite learning algorithms, classification and recognition of myocardial ischemia by deep learning, and Web system assisting doctor diagnosis, which lays the foundation for the construction of serum electrolyte disorder scientific research data center. In order to explore this relationship, without artificially extracting features, a deep learning model of convolution and long-term and short-term memory circulation neural network cascade was proposed to determine the positive or negative myocardial ischemia by classifying serum disorders. Conduct clinical experiments, including patients with suspected coronary heart disease and coronary angiography as the research object, taking coronary angiography results as the detection standard. Experimental results show that the model has an accuracy of 89.0% for detecting myocardial ischemia, a sensitivity of 91.7%, and a specificity of 81.5%. A linear combination model of CNN and LSTM is proposed to classify and recognize serum electrolyte disorders. Determine the learning theory to dynamically model the ST-T segment in the ECG to obtain serum electrolyte disturbance, which more vividly shows the changes in electrical information under myocardial ischemia. In order to reveal the relationship between serum electrolyte disturbance and myocardial ischemia, this paper builds a neural network model to learn and train serum electrolyte disturbance data to realize the classification of positive or negative myocardial ischemia. Tests on serum electrolyte disturbance data collected in clinical experiments show that this model can better achieve early detection of myocardial ischemia.

INDEX TERMS Deep learning, serum, electrolyte disturbance, clinical analysis.

I. INTRODUCTION

Sodium, potassium, chlorine, calcium, phosphorus, magnesium and other electrolytes are mainly present in various tissues of the human body in the form of ions [1]–[5]. Together with proteins, they maintain the osmotic pressure of tissue cells and play an important role in the movement and retention of body fluids [6]. Sodium participates in the formation of various secretions of the human body and plays an important role in maintaining the normal function of nerves and muscles [8]. Potassium not only participates in the metabolism of proteins and sugars in the cell, but also maintains the excitability of nerves and muscles together with calcium and chlorine, and coordinates the contraction and relaxation of normal myocardium [9]. Chloride ions mainly from hydrochloric acid with hydrogen ions, promote the absorption of iron in the body, and active amylase, inhibit the growth of bacteria in the stomach [10]. Calcium in the blood plays an important role in maintaining the content of bone salt in the bones, blood clotting process and neuromuscular

The associate editor coordinating the review of this manuscript and approving it for publication was Yizhang Jiang.

excitability [11]. Calcium in the cell fluid acts as a second messenger and plays many important physiological roles in signal transduction. Muscle calcium in can start the contraction of skeletal muscle and cardiologist [12]. In addition to constituting bone salt components and participating in bone formation, phosphorus is also a component of important biological molecules such as nucleic acids, nucleotides, phospholipids, and coenzymes. Many biochemical reactions and metabolic adjustment processes require the participation of phosphate. More than half of magnesium are deposited in bone and have a sedative effect on nerve and muscle excitability. It is a cofactor for various enzymes [13]–[16]. It participates in all biochemical reactions that require ATP. It also has the maintenance of the stability of the DNA double helix, participation in the activation of amino acids. The important role of ribosome circulation transit peptide and ribosome translocation. Various electrolytes play an important role in maintaining the relative stability of the body's environment and maintaining the body's normal life activities [17]–[21]. When the electrolyte is disturbed, the body will have various clinical reactions. Clinical observation found that patients with liver cirrhosis have a variety of electrolyte disorders, and is closely related to their complications and prognosis [22]–[26].

The natriuretic peptide family is a family of structurally related peptides, including atrial natriuretic peptide, B-type natriuretic peptide and C-type natriuretic peptide [27]–[29]. It is a type of biomarker that is secreted as the myocardial wall tension increases to counteract the effects of the renin-angiotensin-aldosterone system and the sympathetic nerve [30]. ANP has the effect of dilating blood vessels and diuretics [31]. Nishi *et al.* found that most of BNP is secreted by ventricular myocytes [32]. The precursor of BNP is composed of 108 amino acid peptides. When the pressure increases or the volume of the ventricle increases, it changes with the change of the ventricular wall tension [33]. Promote the production of BNP with 32 amino acids from the C-terminus and B-type natriuretic peptide of 76 amino acids at the N-terminus [34], [35]. Natriuretic peptides mediate physiological effects through natriuretic peptide receptors, including increasing glomerular filtration, reducing sodium water reabsorption, reducing myocardial oxygen consumption, dilating blood vessels, and inhibiting myocardial weight antagonism through collagen synthesis and cell hypertrophy Structure [36]. BNP and NT-proBNP levels in patients with HF are elevated [37]. In the early stages of chronic heart failure, elevated BNP and NT-proBNP levels may play an important role in maintaining water and sodium balance and maintaining hemodynamic stability. As the disease progresses, the beneficial effects of BNP and NT-proBNP diminish, leading to water and sodium retention and adversely affecting the heart. Therefore, the increased levels of BNP and NT-proBNP can reflect the severity of left ventricular dysfunction, which increases as the disease progresses [38]. The decision tree algorithm is a machine learning algorithm. The generation algorithm mainly includes CART, ID3, Random Frost, C4.5, C5.0, and others. It is mainly used for classification and prediction, and is based on actual data. Different decision trees are used the method is also different [39]. Compared with other classification algorithms, decision trees are more intuitive and easier to understand. This algorithm can process and classify fuzzy data to generate a prediction model [40]. In recent years, the decision tree algorithm has been widely used in the predictive diagnosis and treatment of diseases in the field of biomedicine. In predicting the incidence of stroke, K-nearest neighbor and C4.5 decision tree has played a role [41], The diagnosis and prediction model of type I diabetes was developed to solve the problem of young people who missed using insulin to lose weight [42]. Some researchers also use multi-layer perception decision tree algorithm to assist clinicians in diagnosis and treatment, and decide the method of treatment of breast cancer [43].

Li *et al.* proposed a heartbeat classification method based on 1D convolutional deep neural network. It first divided heartbeats into 5 categories, and the overall classification accuracy of the 5 categories reached 98.8%. Then it is further divided into two major categories, VEB and SVEB, and the recognition accuracy of the two categories is 99.0% and 97.6%, respectively [44]. Knier *et al.* also analyzed the two major categories of VEB and SVEB, using stack noise reduction automatic coding network and artificial correction of uncertain heart beats, and achieved a recognition accuracy of 99.7% [45]. The accuracy has been improved. Although various heartbeat classification algorithms have been developed, the impact of high noise and complex variability of heartbeat morphology on the stability of the algorithm has not been well resolved [46]–[52].

The decision tree algorithm is a relatively complete data mining algorithm. In the clinic, the hospital's electronic system can intuitively reflect the changes of the patient's clinical indicators, and it also implies other information, such as the risk factors of the disease and the interconnection between the diseases [53]. Now, more and more intelligent technologies have been used in medicine [54]–[63].

In summary, the changes in serum sodium, chloride, and potassium levels have played an important role in the occurrence and development of heart failure caused by various causes, but whether it is closely related to different types of HF is unclear. Due to the particularity of HF patients, subtle changes in serum iron levels may play a more important role in patients with heart failure. The disadvantage is that the influence of high noise and complex variability of heart beat shape on the stability of the algorithm has not been well solved. At present, the determination of serum ions is relatively simple, and accurate results can be obtained in different levels of hospitals. How to use serum iron levels to simplify the determination of the severity and prognosis of HF patients has high clinical value. Therefore, by analyzing the relationship between natriuretic peptides, serum ions and HF and different types of HF patients, we established a standard for serum ions to predict the prognosis of heart

TABLE 1. Electrolyte disorders.

Category	K		Na		Cl	
Number of cases (n)	Rise	Reduce	Rise	Reduce	Rise	Reduce
	1	30	2	48	8	39
Percent Age (%)	0.6	17.96	1.2	28.74	4.79	23.35
A	0	5	1	1	0	0
B	0	14	1	19	6	17
C	1	11	0	28	2	22
Category	Ca		P		Mg	
Number of cases (n)	Rise	Reduce	Rise	Reduce	Rise	Reduce
	0	40	5	5	1	5
Percent Age (%)	0	23.95	2.99	2.99	0.60	2.99
A	0	2	0	0	0	0
B	0	19	3	3	0	3
C	1	19	2	2	1	2

failure, and provided a theoretical basis for the diagnosis and treatment of HF patients.

II. DEEP LEARNING MODEL OF SERUM ELECTROLYTE DISTURBANCE

A. DATA SOURCES

A total of 169 patients with heart failure from May 2018 to June 2019 were selected as the heart failure group [45]. The heart failure group is divided into heart failure according to the classification criteria of ejection fraction and heart failure. It is divided into heart failure with reduced ejection fraction (HFrEF), heart failure with median ejection fraction (HFmrEF), and heart failure preserved heart failure (HFpEF). The three groups were labeled A. B, and C in sequence, and 49 non-heart failure patients who was hospitalized in the geriatrics department at the same time was selected as the non-heart failure group.

In this study, a total of 167 patients with cirrhosis in our hospital were collected. The patients were 20-76 years old, with an average age (50.93 $\pm$ 11.05) years. 125 male patients (74.90%), aged 20-76 years old, average age (50.20 $\pm$ 10.86) years old, 42 female patients (25.10%), aged 26-74 years old, average age (53.12 $\pm$ 11.44) years old, male and female patients Ratio 2.98: 1. Among 167 cirrhotic patients, 136 patients (81.43%) had post-hepatitis B cirrhosis, 5 patients (2.99%) had cirrhosis after viral hepatitis C, and 14 had alcoholic cirrhosis (8.38%), 6 patients with cirrhosis after autoimmune hepatitis (3.59%), 1 patient with cirrhosis after hepatolenticular degeneration (0.60%), and 5 patients with unexplained cirrhosis (2.99%). Of the 167 patients, 19 (11.38%) had hepatic encephalopathy, 25 (14.97%) had upper gastrointestinal hemorrhage, and 4 (2.40%) had hepatic kidney syndrome (spontaneous bacterial). There were 2 cases (1.20%) of peritonitis and 37 cases (22.16%) with primary liver cancer. The mean value of the Child-Pugh classification score of 167 patients with liver cirrhosis was 8.59 2.089, including 27 patients with grade A (16.17%), 86 patients with grade B (51.50%), and 54 patients with grade C (32.33%). As showing in Table 1. Of the 20 patients in this group, 7 (35%) had varying degrees of consciousness disturbance, 10 (50%) had limb weakness, 13 (65%) had varying degrees of speech impairment, and 8 (40%) had swallowing Difficulties, silence in 6 cases (30%), brusqueness in 5 cases (25%), limb tremor in 2 cases (10%), hand-foot movement in 1 case (5%), and urine in 3 cases (15%) Dyspepsia, 4 patients (20%) had abnormal mental behavior, 2 patients (10%) had seizures, and 1 patient (5%) had unstable walking. Physical examination revealed that 12 patients (60%) had increased limb muscle tone and 5 patients (25%) had positive pathological reflexes.

Of the 20 patients in this group, 16 patients (80%) had serum electrolyte disturbances. Among them, there were 13 cases of hyponatremia (65%), 11 cases of hypokalemia (55%), 2 cases of hypernatremia (10%), and 1 case of hypochloremia (5%). Electrolyte status of 2 patients (10%) was unknown. 2 patients (10%) had normal serum electrolytes. 1 patient with long-term use of indapamide to control blood pressure developed hyponatremia, hypokalemia, and hypochloremia. The serum electrolytes in the external hospital were as low as: potassium: 2.97mmol / L, sodium: 99mmol / L, chlorine: 55mmol / L. Among them, 2 cases (10%) were rapid increase in blood sodium concentration, and serum sodium concentration increased more than 10mmol / L within 24 hours of rehydration [36], 2 cases (10%) were rapid decrease in blood sodium concentration, 1 patient within 1 day Reduced blood sodium concentration by 15 mol / L, 1 patient reduced blood sodium concentration by 11 mol / L in 1 day, 9 patients (45%) had an unknown fluid replacement rate (history of sodium supplementation and potassium supplementation in other hospitals), 3 patients (15%) Sodium supplementation at normal speed (the blood sodium concentration does not exceed 10 mol / L within 24 hours of fluid replacement).

B. DEEP LEARNING ALGORITHM MODEL

As showed in Figure 1, the LRCN model directly connects the cyclic sequence model to the convolutional network model

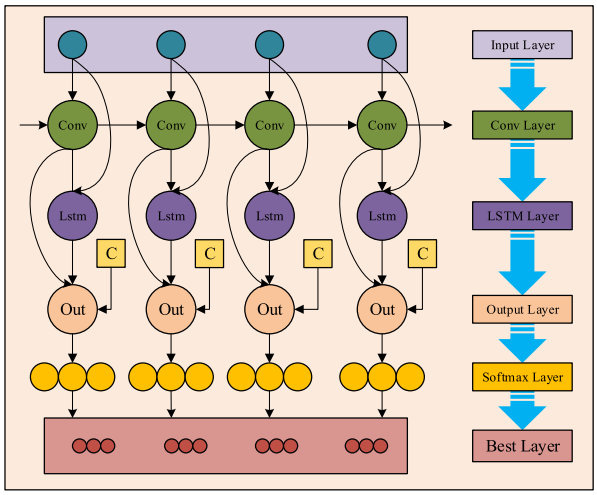

FIGURE 1. Conv-LSTM model network structure diagram.

for joint training to achieve object detection and motion recognition in video images. This is a spatial and temporal depth of the two models [46]. Fusion, this end-to-end model training is flexible enough to handle various visual tasks involving timing sequence. First, the input video image is intercepted frame by frame to obtain the image frame sequence, and then passed into the LRCN model. CNN performs a convolution operation on each image in the image frame sequence to extract the features of the image [47]. These features are based on the original frame sequence. Arranged in sequence to form time series data, and then input these time series data into the LSTM model for training, each LSTM unit will output the corresponding classification results, and finally use a comparison strategy to analyze the classification results and draw conclusions. The model makes full use of CNN's good image processing advantages and LSTM's long-term memory of the dependency between adjacent data of time series data. It has a good effect on the behavior detection and description of video images. It is a combination of CNN and LSTM a good attempt to build a complex network structure.

The Conv-LSTM model is proposed to solve the classification problem of human behavior data collected by multi-axis sensors. It is a deep neural network composed of multiple CNN layers and LSTM layers. First, the multi-dimensional time series data collected by the sensor generate more abstract features after CNN operation. These convolutional layers are only processed in the time direction, so the dimension of the input data does not decrease after convolution, and the convolution kernel is along each the data of the channel is convoluted. The convolution model is also a typical design method, including several convolutional layers and pooling layers, and uses ReLU nonlinear function as the activation function. Then these features can be obtained after the LSTM network training, and the time dynamic features can be obtained [48]. The activation function uses the trash function, and finally the classification results are obtained through the Softmax layer. The number of CNN layers and LSTM layers selected by this model is obtained based on actual experience, but generally speaking, Conv-LSTM first performs convolution processing on the entire time series data, and then enters the feature map sequence into the LSTM network to capture the dynamics in time Feature, the model fully exploits the long-term dependence features of time series data, and provides us with good ideas by linearly combining CNN and LSTM. The data between multiple channels of sensors often do not interfere with each other, and the three values of CDG at each time point determine the spatial position, so it is not necessary to use one-dimensional convolution operations to move along the time axis. Shortening the sequence length can increase the dimension, and can extract more abstract features [49]. Then enter the LSTM network to extract these sequence feature data, and finally obtain the probability distribution through the Softmax layer to determine whether the patient has myocardial ischemic disease. Therefore, combining the above two models, the Conv-LSTM model is slightly adjusted to propose the network structure used in this paper.

RBF neural network is a radial basis function neural network. It is an efficient feed-forward neural network. It has the best approximation performance and global optimal characteristics that other feed-forward networks do not have. It has a simple structure and fast training speed. At the same time, it is also a neural network model that can be widely used in the fields of pattern recognition and nonlinear function approximation.

$$k_{nn}(x) = \sum_{i=1}^{N} w_i s_i(x) = W^T S(x) \tag{1}$$

$$H = [\mathrm{h}_1, \mathrm{h}_2, \ldots, \mathrm{h}_N]^T \in R^N \tag{2}$$

The radial basis transformation function is a non-negative non-linear function that is radially symmetric to the center point and decay. In this paper, Gauss (Gauss) function is used as the hidden layer activation function of the RBF neural network. It has the advantages of simple expression, good smoothness, good resolution, etc. It is the most widely used activation function, as follows:

$$G_i(\|x - \ell_i\|) = \exp\left[\frac{-\|x - \ell_i\|^2}{\eta_i^2}\right], \quad i = 1, 2, \ldots, N \tag{3}$$

$$\ell_i = [\ell_{i1}, \ell_{i2}, \ldots, \ell_{i3}]^T \tag{4}$$

When a radial basis neural network with a sufficient number of nodes N and an appropriate center point and width is selected so that the neurons are evenly distributed, an arbitrary continuous function defined above can be approximated with arbitrary accuracy:

$$b(x) = W^{*T} S(x) + \varepsilon(x), \quad \forall_x \in \Omega_x \tag{5}$$

Mt is the ideal constant RBF neural network weight vector, and S is the approximation accuracy of the neural network.

Assuming existence, for any such that it is the minimum, the following formula (6):

$$M^* = \arg\min \left\{ \sup_{x \in \Omega_x} \left| b(x) - W^T S(x) \right| \right\} \tag{6}$$

RBF neural network is widely used in system identification and modeling of nonlinear systems due to its ability to learn complex input and output mapping and excellent approximation ability, especially based on Lyapunov stability theory, it is widely used in adaptive control And pattern recognition, but a large number of references are only based on the stability analysis of the system, to ensure that the state tracking trajectory and the weights of the neural network converge within the specified range, and there is no guarantee that the weights learned by the neural network will approximate the dynamics of the actual system. Research in the field of system identification has found that when the Persistence of Excitation (PE) is satisfied, the parameters in the estimated dynamic system model converge to the real system. However, the PE condition of the nonlinear system is difficult to verify in advance, and its definition is as follows:

$$\partial_1 J \leq \int_{t_0}^{t_0+T_0} S(\tau) S(\tau)^T d\tau \leq \partial_2 J, \quad \forall_{t_0} \geq 0 \tag{7}$$

$$\partial_1 \leq \int_{t_0}^{t_0+T_0} \left| S^T(\tau) c \right| d\tau \leq \partial_2, \quad \forall_{t_0} \geq 0 \tag{8}$$

According to the above definition, a more general equivalent definition is given to satisfy the identification of continuous and discrete RBF networks. Let be a Boreal measure, given a uniformly bounded piecewise continuous vector function, if there is a normal number, as follows:

$$\begin{aligned} \partial_1 \|c\|^2 &\leq \int_{t_0}^{t_0+T_0} \left| S^T(\tau) c \right|^2 d\nu(\tau) \\ &\leq \partial_2 \|c\|^2, \quad \forall_{t_0} \geq 0, \ c \in R^n \end{aligned} \tag{9}$$

Consider all periodic (regressive) trajectories x (t) with arbitrary period To, if x (t) exists: [0, ∞)+ 2CR is a continuous map, and x (t) remains in the compact set 2CR'' Then, for the RBF neural network W_1 S (x), if the center points of the neurons are evenly distributed in the compact set S_2 region, the regression sub-vector S <(x) along the trajectory x (t) can satisfy the PE condition and determine the learning The theory generalizes and relaxes the ε-neighborhood must be less than the center distance of two neurons as:

$$\phi \geq \sqrt{qh}\sqrt{q}/2^* \min_{i \neq j} \left\| \ell_i - \ell_j \right\| > 0 \tag{10}$$

$$D_\varepsilon(x(t)) = \left[s\left(\left\| x(t) - \ell_{j1} \right\| \right) \right] \tag{11}$$

It is determined that the learning theory relaxes the restriction that the signal must pass through the small neighborhood of each neuron, so that the neurons along most trajectories or quasi-period trajectories along the trajectory can meet the PE condition, so as to achieve local accurate construction of the dynamic system.

C. ANALYSIS AND DESIGN OF DEEP LEARNING SYSTEM FOR SERUM ELECTROLYTE DISTURBANCE

Clinical research is inseparable from data collection. When initially applying the definite learning theory to the early diagnosis of myocardial ischemia, it is necessary to go to the partner hospital to collect ECG data and manually enter the medical record. Patients cause a lot of inconvenience. Subsequently, based on the B / S architecture, a remote myocardial ischemia workstation system was developed to facilitate doctors to quickly analyze and diagnose ECG data and medical records files, but it is also necessary to obtain data through doctors and institutional personnel, and then manually analyze and organize medical records files and enter the system [50]. A lot of manpower and material resources were wasted. However, with the further promotion of clinical trials in multicenter hospitals to verify the effectiveness of diagnosis, the traditional data collection method obviously cannot meet the requirements. Clinical datum has the characteristics of retrospective research and needs to accumulate and improve medical record information for a long time. Its main sources are the hospital's Electronic Medical Record (EMR) and medical image archiving and communication system (PACS). There are paper medical records and Excel documents that doctors usually save. Clinicians often hope to solve the statistical analysis of data with the least amount of time, so that the diagnostic system can quickly calculate to meet the scientific research requirements of clinicians.

This paper focuses on the current informatization construction in the central hospitals with electronic medical records as the core, integrates various heterogeneous data in the Hospital Information System (HIS) and data collected by on-site ECG acquisition equipment, and uses definite learning theory to extract myocardium The features related to ischemia are then designed to be classified for doctors to use, and a medical system centered on the auxiliary diagnosis of myocardial ischemia is designed, including the data layer, the calculation layer and the application layer. Atlas analysis and big data analysis data mining and other tasks, the system architecture is shown in Figure 2.

The data layer does not change the existing hospital information system, transmits the single-node medical raw data in the HIS through the network and distributed storage to the Hadoop-based data center, the structure and unstructured data in various heterogeneous databases. It is saved on Linux cluster nodes through file partitioning; the computing layer is to perform resource scheduling and calculation allocation through Yarn to realize the distributed calculation of learning ECG data, and then store the results in HDFS by building Mahout and Tensor flow. Can perform effective data analysis on the data in the data center and provide decision information for the application layer. Application layer users can use the browser's operation interface to call the business API interface to view the auxiliary diagnostic results and data statistical analysis results, and control the calculation through interface interaction. The layer implements data analysis and data layer access to data.

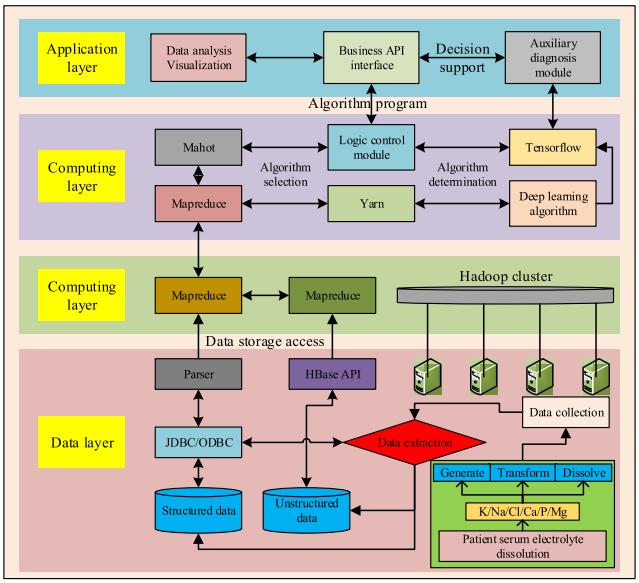

FIGURE 2. Architecture diagram of deep learning system for serum electrolyte disorder.

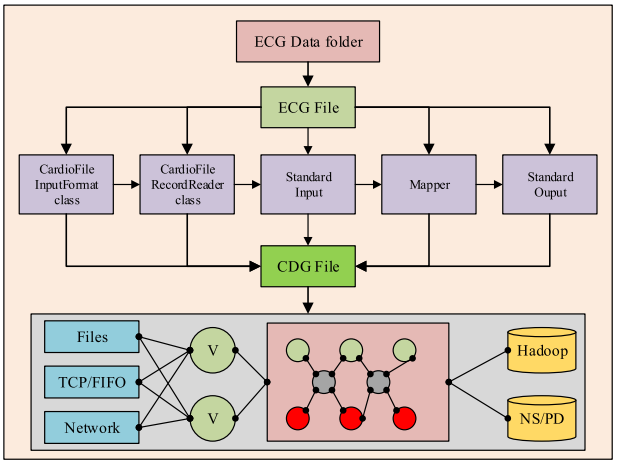

FIGURE 3. Flowchart of generating CDG from ECG distributed computing based on Hadoop stream.

Hadoop Stream will use the class to block the input file and process the block content by line at the same time. The key is the beginning of the line and the offset of the entire file, and the value is the content of the line. However, the 12 leads of ECG data are an inseparable whole. ECG data is often stored in files in columns, so you need to customize the class file and a class file to determine the end line of the file and record the complete record of each block. The content is then passed into the Mapper program for processing. Figure 3 is a flow chart of generating CDG from ECG distributed computing based on Hadoop Stream.

The definite learning algorithm of the computing layer in myocardial ischemia diagnostic system interacts with the application layer through a Python script program. The application layer background program provides an interface to control the calculation layer algorithm execution. The computing layer uses Python scripts to call the Linux Shell to control the execution of Hadoop cluster tasks in this way, the application layer is focused on business development, and the calculation layer is focused on algorithm design and calculation, which achieves a good decoupling between the two. It should be noted that the HDFS output folder of Hadoop must remain unique, otherwise the calculation will fail. In order to ensure concurrent access to the system, the combination of thread number and UUID can ensure that the output folder name is unique, so that even if the data are placed in different folders, the same data double calculation problem can be avoided.

TABLE 2. Diagnostic criteria for framingham heart failure.

Main diagnostic criteria	Secondary diagnostic criteria
Paroxysmal dyspnea at night	Cough at night
Lung chirp	Ankle edema
Jugular vein dilation	Hepatomegaly
Enlarged heart	Difficulty breathing after activity
Acute pulmonary edema	Pleural effusion
Increased venous pressure	Tachycardia (> 120 beats / min)
Third heart sound	Reduced vital capacity to 1/3 of maximum vital capacity

D. RESEARCH ON CLINICAL ANALYSIS STANDARDS

The diagnosis of heart failure needs to meet 2 major criteria or 1 major criterion plus 2 minor criteria, as detailed in Table 2 below.

Acute coronary syndrome within 30 days; heart failure patients with severe hepatic and renal insufficiency; benign or malignant tumors and hematological diseases; chronic obstructive pulmonary disease; patients with acute stroke and heart disease within 3 months Surgical patients. SPSS26.0 statistical software for descriptive statistical analysis and correlation analysis. The measurement data conforming to the normal distribution are expressed by $x \pm s$, and the non-normal distribution is described by M (Q1-Q3); the count data are expressed by percentage. One-way analysis of variance was used to compare the measurement data that satisfy the normal distribution among multiple groups. Compared with the t-test method using independent samples between the two groups, a non-parametric test was adopted for disobeying the normal distribution. $P < 0.05$ indicates that the difference is statistically significant.

Effectiveness indicators: The main outcome indicators include the total clinical effectiveness (total effective = significant efficiency + effectiveness). Significant effect: heart function is improved by more than two levels, and symptoms and signs are significantly improved; effective: heart function is improved by one level, but insufficient at both levels, symptoms and signs have improved; ineffective: the heart function

is not improved by one level or the condition is aggravated or died. The efficacy of TCM syndromes is the same as the study. BNP, LVEF and 6MWT are an index for evaluating exercise endurance of CHF patients. It requires patients to walk as fast as possible in a straight corridor, measuring the 6-minute walking distance. 6MWT <150 m is severe cardiac insufficiency, 150 ∼ 425 m is moderate, 426 ∼ 550 m is mild. Effective: 6MWT increased by 1 grade; ineffective: 6MWT was not significantly improved; worsened: heart failure worsened or even died.

They mainly collected electrocardiograms of patients with normal ECG and suspected myocardial ischemia and recorded complete medical records of patients. The patient's ECG is collected before the patient undergoes coronary angiography, and coronary angiography results are used as training labels for supervised learning and the accuracy of model classification is calculated. The patient's medical record data is obtained by the hospital's HIS system, and the XML file is directly output by the electrocardiograph. The image data is obtained by the hospital's imaging department and the corresponding image file is obtained. Stored in HDFS, CDG data is finally obtained through calculation at the computing layer. In order to further reveal the relationship between CDG and myocardial ischemia, the clinical trials strictly controlled the selected cases, excluding many patients with unrelated causes of myocardial ischemia, experimental collection equipment and instruments. After filtering to remove various noise, ECG data is then subjected to ST-T segment interception and converted into ST-T vector loops. After determining the features to learn and extract the CDG, these calculation processes are quickly completed in batches on the Hadoop platform, greatly reducing the generation time of training data. In this experiment, 1714 complete medical records and CDG data were collected. These patients were diagnosed with myocardial ischemia after coronary angiography. 1236 of them were diagnosed with myocardial ischemia, that is, coronary stenosis exceeded 50%, while 478 subjects were healthy and normal. CDG data of all subjects are normalized by the maximum and minimum method. The CDG data length is 2000. After training by neural network, it is compared with the label of the data itself. Generally speaking, as the number of training increases, the verification and test results of the neural network oscillate around a fixed value. After 6000 iterations, the model's fitting degree has basically stabilized. The experiment uses the sensitivity and specificity commonly used in medicine to evaluate the effect of combining CNN and LSTM to detect negative and positive myocardial ischemia. Sensitivity is the percentage of specific disease that is actually classified by the model and actually identified by the model. Specificity) refers to the percentage of healthy and disease-free models that are correctly identified as disease-free. Accuracy refers to the percentage of all data correctly classified by the model. The calculation formula is as follows:

$$A = \frac{TP}{TP + FN}(\%) \tag{12}$$

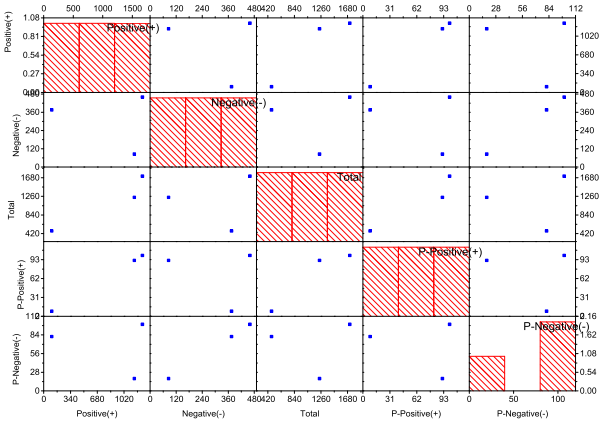

FIGURE 4. Deep learning model detects myocardial ischemia.

$$B = \frac{TN}{TN + FP}(\%) \tag{13}$$

$$C = \frac{TN + TP}{TN + FP + TP + FN}(\%) \tag{14}$$

TN means true negative, refers to the number of non-myocardial ischemia detected by non-patients; TP means true positive, refers to the number of patients diagnosed with myocardial ischemia by this model; FN indicates false negative, refers to patients diagnosed with myocardial ischemia Is the number of non-patients; FP means false positive, which refers to the number of non-myocardial ischemic patients diagnosed as myocardial ischemic patients.

III. RESULTS ANALYSIS

A. THE RESULTS OF DEEP LEARNING MODEL TO DETECT MYOCARDIAL ISCHEMIA

After the training of the neural network model, CDG data of all subjects were compared with the results of coronary angiography diagnosis. The average value was obtained after multiple experiments. The experimental results are shown in Figure 4. In CDG data of all patients, the accuracy rate of the neural network model for detecting myocardial ischemia is 89.0%, the sensitivity is 91.7%, and the specificity is 81.5%. However, because the collected data are not very balanced, the probability that the neural network determines that the myocardial ischemia is positive is higher than that of the negative, and the resulting sensitivity is significantly higher. In the early stage, the accuracy of detection of 421 patients with suspected coronary heart disease with roughly normal ECG by extracting two indexes of temporal heterogeneity and spatial heterogeneity was 84.6%. The model proposed in this paper improves the accuracy rate. In the future, the clinical trials will be further promoted, and more complete myocardial ischemia data will be collected from more subjects. The combination of CNN and LSTM for CDG classification and identification will be an effective way to detect positive or negative myocardial ischemia.

Each loop in the CDG loop corresponds to the ST-T segment. The healthier the heart, the higher the degree of

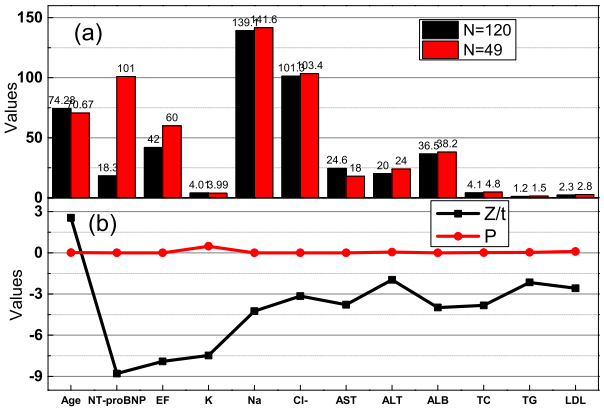

FIGURE 5. Comparison of baseline data between heart failure group and non-heart failure group.

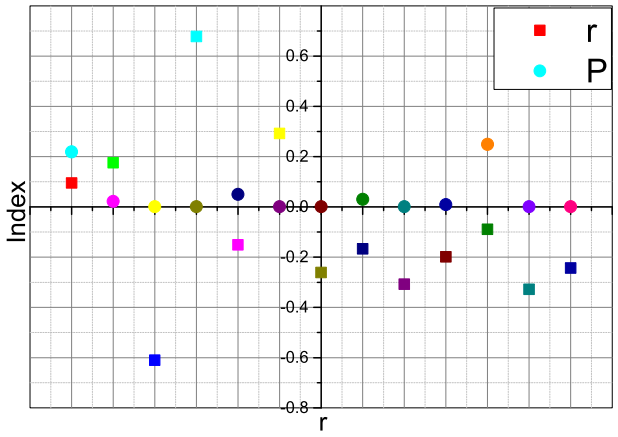

FIGURE 6. Correlation analysis of various indicators of serum electrolyte disturbance.

coincidence between the loops, but it is not completely coincident. This change is recorded by CDG. CDG loops of healthy people are obviously coincident, and the trajectory is relatively clear, showing a ring shape. However, CDG loops of myocardial ischemia patients are clearly separated, and the trajectory is relatively scattered. These morphological differences can be found by qualitative analysis. Morphology of CDG is related to myocardial ischemia. This system does not require manual design of the classifier or feature extraction or selection according to the CDG morphology. Using neural networks to automatically extract intrinsic features for classification can obtain a model with high accuracy. As the amount of data increases, further research in more hospitals and different data sets can achieve better system performance. Further, we propose a new method of automatically diagnosing myocardial ischemia. By modeling the original ECG signals to generate CDG signals, and then learning the CDG signals through the system model, we can finally perform early diagnosis of myocardial ischemia.

In the comparison between the heart failure group and the non-heart failure group, the P values of age, NT-proBNP, LVEF, Na +, Cl-, LDL, AST, ALT, ALB, TC, TG were all <0.05, and the difference was statistically significant. According to correlation analysis, the P values of age, EF, NT-proBNP, AST, TC, TG, ALB, LDL, Na +, Cl- are all less than 0.05, indicating that their correlation with heart failure is shown in Figure 5.

As showed in Figure 6, the correlation analysis of various indexes of serum electrolyte disturbance.

Sodium ions (Na +) are essential nutrients for the human body. They are the most important extracellular cations outside the body, generating osmotic pressure and maintaining the balance of water inside and outside the cell. Patients with heart failure often have sodium in disorders due to decreased renal perfusion and excessive activation of neurohumoral factors, which is also an important reason for choosing sodium ions as clinical research indicators.

This study found that there is a significant difference in sodium ion levels between elderly heart failure and non-heart failure patients. In patients with heart failure, sodium ion levels are significantly reduced. Therefore, this study introduces sodium ions as a risk factor for heart failure. In this study, the decision tree algorithm was used to find that when Na + $<$139mmol / L. Heart failure is more likely to occur. Therefore, when Na + $<$139mmol / L, heart failure is more likely to occur. The results obtained in this study suggest that in elderly patients with heart failure or suspicious heart failure, monitoring sodium ion levels, 139mmol / L may be a valuable node for joint judgment of elderly heart failure. Therefore, in the clinic, even if the patient's serum sodium ion level is in the low normal range, the risk of heart failure may increase. Therefore, in the clinical management of elderly patients, sodium cannot be strictly limited. How to judge the time to supplement sodium in an appropriate amount for elderly patients to avoid blood sodium at a low normal value or below the normal value can reduce the risk of heart failure. This study found that there is a difference in Cl- levels between elderly heart failure and elderly non-heart failure patients. Cl- is negatively correlated with the occurrence of heart failure. That is, Cl- levels are reduced, and the risk of heart failure may be greater. In the heart failure prediction model established by random forest, it can also be seen that Cl- also plays a role in predicting the occurrence of heart failure. Cl- is indeed an influencing factor of heart failure, and it has a certain auxiliary diagnosis for our clinical the role.

B. ANALYSIS OF AUTOMATIC RECOGNITION OF SERUM ELECTROLYTE DISTURBANCE

In the experiment, we constructed 33,950 heartbeats from different people. Among them, 22350 heartbeats are used as training set, which includes 8000 N, 5500 LBB, 4200 RBB, 1320 PVC, 1030 AP and 2300 P. Another 11600 heartbeats were used as the test set, which included 3600 N, 2400 LBB, 2400 RBB, 1150 PVC, 850 AP and 1200 P. For the superimposition of all six types of heartbeat data in the test set, it can be seen from the figure that although it is the same type of heartbeat data, there are also large

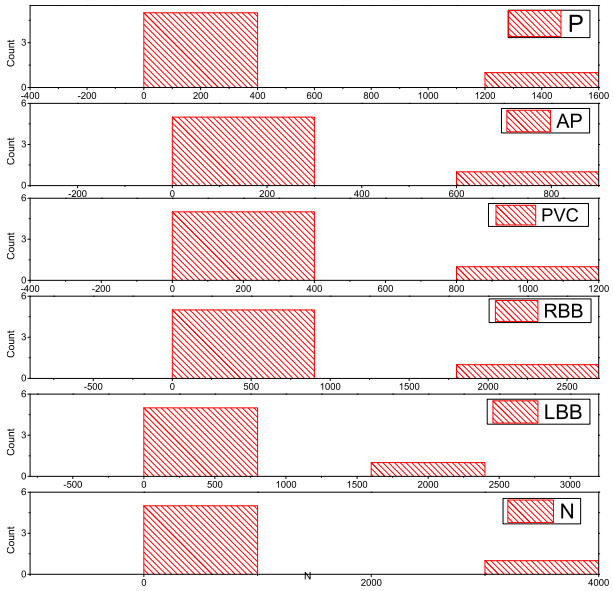

FIGURE 7. Results of automatic recognition of serum electrolyte disturbance.

differences in morphology (such as b and d subgraphs), and the similarity of the same type of heartbeat itself The main reason for the unstable heartbeat automatic recognition algorithm. N and P heartbeats have good consistency in shape. The matching matrix of the six types of heartbeats is shown in Figure 7. The row represents the algorithm to obtain the classification results of six types of heartbeats, the columns represent the actual heartbeat classification results, and the data on the diagonal are the number of correctly detected heartbeats in each type of heartbeat. It can be seen from the data in the table that there are more misjudgments between the N heartbeat and the AP heartbeat. The N heartbeat is easily recognized as an AP heartbeat, and the AP heartbeat is also easily recognized as an N heartbeat. The main reason is that the N heart beat and the AP heart beat are similar in shape, and the significant difference is that the P wave shape changes in the heart beat, and the P wave is a wave with a small amplitude in the heart beat, and the amplitude change of the P wave is different in different individuals, so it is easy Confusion between N and AP heartbeats. The LBB and PVC heartbeats themselves have various morphological changes, and there are certain similarities between the two types of heartbeats, both of which are reflected in the changes in the QRS complex and ST segment morphology, so it is easy to cause misjudgment between the two. RBB heartbeats are also similar in shape to PVC heartbeats, and can also cause false recognition. The P heartbeat itself has a good form consistent and is quite different from other heartbeats, so the recognition rate of the P heartbeat is the highest.

The statistical results of S and P of the six heart beats are shown in Table 2-4. From the data in the table, it can be concluded that the sensitivity of the P heart beat is the highest, which is 100%. Prediction of RBB heart beat is the highest

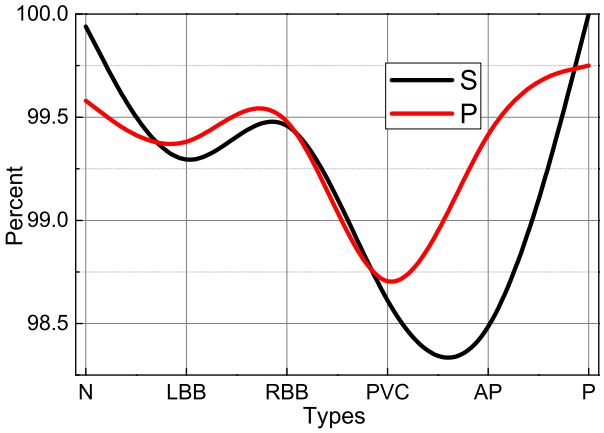

FIGURE 8. Statistics of sensitivity S and prediction P.

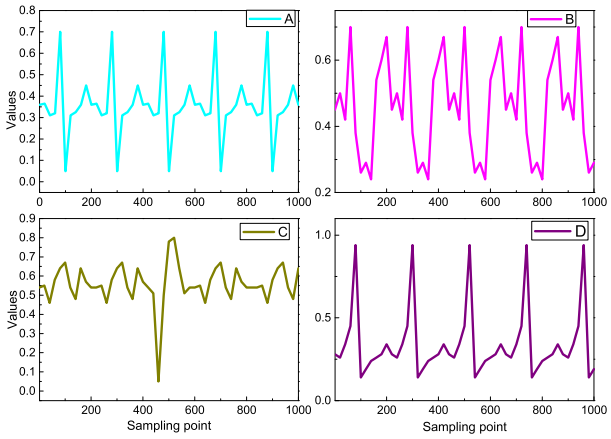

FIGURE 9. Unrecognized SCD signal form.

at 99.87%. The average predictability of the six heart beats is slightly higher than the average sensitivity. P and S have good stability for 6 types of heart beats, and are less affected by changes in heart beat patterns. As showing in Figure 8.

The connection spectrum radius of the reserve pool, the input scaling ratio and the leakage rate are the main parameters of the ESN network. Value selection has a great influence on the SCD recognition results. Figure 9 shows the SCD recognition results when the three parameters are changed. S) and predictability (P) as measurement indicators. From the data in the figure, it can be seen that as the connection spectrum radius of the reserve pool decreases, its sensitivity and predictability increase, and the change is more obvious when it decreases from 0.1 to 0.01. When decreasing, S and P no longer increase, but on the contrary there is a significant decrease, so the final setting is 0.001. The input scaling ratio controls the scaling of the input weight matrix.

Too large a scaling ratio will obviously reduce the recognition ability of the network, and too small a scaling will obviously reduce the recognition sensitivity. Finally, 0.1 is selected. The leakage rate in the formula (6) controls the speed of the dynamic update of the reserve pool. As the value

of increases, the accuracy of SCD identification gradually improves until its value is close to 1, after continuous testing, it is finally set to 0.99.

Figure 9 shows the unrecognized ECG signal form in the SCD test data set. Figure (a) has a relatively sharp QRS wave group, and the amplitude of the upper and lower peaks is similar. Figures (b) and (c) have more intense the morphology or RR interval changes, the graph (d) and the CHF signal has a certain similarity. Through statistical analysis of unrecognized SCD signals, it is found that ECG signals with large unrecognized SCD ratios often have strong dynamic characteristics, and there will always be dramatic changes in the shape or period of the signal, accompanied by large amplitude noise.

The purpose of this study is to establish an effective cardiovascular disease monitoring mechanism, use deep learning algorithms to mine hidden cardiovascular diseases in ECG signals and related medical images, and carry out timely intervention and treatment. For high-risk groups, establish a real-time dynamic monitoring and risk warning system to effectively reduce the death rate due to cardiovascular disease. At the same time, it reduces the workload of doctors 'repeated work and reduces the difference of doctors' diagnosis results in different regions.

After SCDHD and NSRD data verification, the signal recognition accuracy 5 minutes before the sudden death reaches 90.88%, and it has a high sensitivity. Knier *et al.* [46] directly analyzed ECG time series signals. By extracting features from wavelet decomposition signals and neural network classification, the average recognition accuracy of SCD signals and normal signals 5 minutes before sudden death reached 95.80%. The analysis method based on the ECG time series signal is relative to the analysis of the HRV signal, and the analysis can be performed directly without knowing the position of the R characteristic wave. The analysis method based on HRV must first accurately extract the position of the R characteristic wave, and then obtain the HRV signal. Before sudden death occurs, the ECG signal shape has a large variability. Accurate extraction of R feature waves is a difficult task. Accuracy of R feature wave extraction will also affect the final recognition effect. In this paper, starting from the ECG timing signal, the deep ESN network is used to classify the 4-second ECG signal without the need to extract the HRV signal, nor the feature extraction and feature screening. Three database data to SCDHD, NSRD and CHFD were used to verify the algorithm, and SCD signal recognition accuracy 5 minutes before the sudden death was 88.90%. The malignant heart failure signal contained in the CHFD database is morphologically closer to the SCD signal, making it more difficult to identify. When we remove CHFD data from non-SCD signals, the test sensitivity reaches 96.64%. As showed in Figure 10, it is a comparison with the experimental results of existing methods.

This chapter mainly studies the SCD intelligent prediction method based on the echo state network, and discusses the difficulties of the SCD intelligent prediction and related

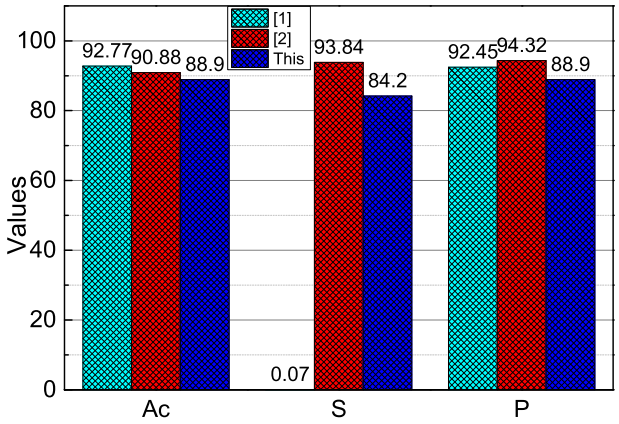

FIGURE 10. Comparison of experimental results with existing methods.

research methods in detail. Accurate prediction of SCD is achieved by constructing an echo state network with a 10-layer series structure. The specific implementation process of the algorithm in this article is introduced in detail, especially the process of data construction. In the experimental results, the experimental results obtained by the algorithm in this paper are given in detail, and the characteristics of the failure to accurately identify the signal are analyzed. The signals within 1-5 minutes before sudden death are analyzed, and the respective prediction accuracy within 1-5 minutes is given. Finally, detailed experimental comparison results are given and detailed discussions are conducted to prove the effectiveness and innovation of the algorithm in this paper.

In this study, some patients with liver cirrhosis developed serum potassium, chloride, magnesium, and pancreatic disorder. The possible mechanism of blood potassium disorder: reduced food intake and gastrointestinal absorption in patients with liver cirrhosis, coupled with impaired liver function, reduced potassium in the body, if there is vomiting, abdominal contamination, clock loss increases. Patients with liver cirrhosis have increased secondary acid sterner, and long-term use of immunosuppressant's can reduce the serum potassium concentration. When enzyme dysfunction occurs on the cell membrane, it will affect the transport of potassium ions, which in turn will affect blood potassium. Patients with liver cirrhosis combined with acidosis, oliguria, gastrointestinal bleeding, use of potassium-sparing diuretics, it can make blood potassium high. Blood Chlorine Disturbance: Patients with liver cirrhosis due to portal hypertension, gastric varices, in order to protect the gastric point membrane and prevent bleeding, taking receptor antagonists and proton fruit inhibitors to reduce gastric acid secretion can lead to lower serum chloride; patients with anions in the body Keeping balance with cations, when the concentration of positive ions such as sodium, potassium, and magnesium changes, negative ions such as chloride ions also change accordingly. The occurrence of blood magnesium disorder is not only related to the patient's low food intake, poor gastrointestinal absorption, vomiting, and increased loss caused

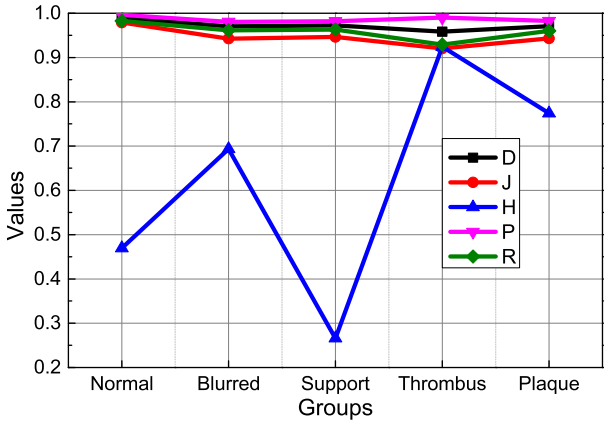

FIGURE 11. Statistics of evaluation index values of intima extraction.

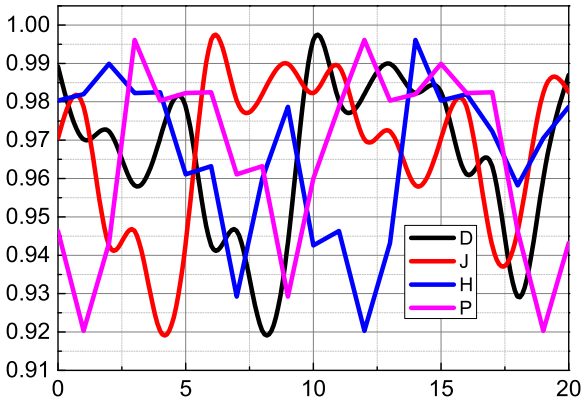

FIGURE 12. Change curve of evaluation index value.

by abdominal bay, but also to the application of diuretics, secondary aldosterone, and long-term use of magnesium-free solutions. Serum ions and serum Korean ions have a mutual treatment relationship with physiological functions. The disorder of blood phosphatidylcholine is related to the disorder of blood scalp. In addition, the possible mechanisms of occurrence are: digestive dysfunction in patients with liver cirrhosis, stomach Decreased, long-term good appetite, inadequate ingestion and absorption disorders, resulting in a decrease in blood. Severe necrosis of liver cells or increased permeability, acidic acid overflow, decreased enzyme activity in the liver, especially decreased permeability, and acidification disorder leads to increased blood pressure. When teratogenic syndrome is oliguria, the excretion of pity is poor, causing an increase in blood levels.

C. EXTRACTION ANALYSES OF CORRELATION OF SERUM ELECTROLYTE DISTURBANCE

In the experiment, we divided the images into five groups according to the characteristics of the algorithm, namely normal, blurred border, stent, thrombus and plaque group. In the normal group, the layered structure of the image is obvious, and there are continuous highlight areas outside the boundary of the intima; the boundary blur group mainly includes the layered structure is not obvious, the gray value between layers is similar, and the boundary is extremely blurred or the boundary is close to the image Marginal; the stent group contains the stent structure; the thrombus group is the presence of obvious thrombus or residual blood in the lumen of the blood vessel; the plaque group is the presence of various types of plaque outside the vascular intima. Each group selects 20 groups of images for analysis.

Figure 11 shows the results of endometrial extraction of five typical images. From top to bottom, they are normal, blurred border, stent, and thrombus and plaque group. From left to right are the original OCT image, the gold standard map (manually segmented), and the algorithm automatically extracts the map. It can be seen from the figure that the algorithm of this paper can accurately locate the boundary position of the intima for five typical images, and has a good agreement with the intima in the gold standard image. In order to more accurately evaluate the effect of the algorithm's intima extraction, we statistically analyzed the average sieve coefficient (D), Jaccard coefficient (J), Hausdorff distance (H), and accuracy of 20 images in each group. And the recall rate (R) and the corresponding mean square deviation. The statistical results are shown in Figure 12. At the same time, the change curves of different images D, J, P and R in the five groups of images are given, as shown in Figure 12, where the red line is D, the blue line is J, the green line is P, and the black line is R. From this we can see that the algorithm of this paper have the best effect on extracting the intima of the normal group of images, and several evaluation indicators have better stability for different images. The main reason is that the normal group of images is relatively simple, and the images have a high degree of similarity, so they have high accuracy and stability. For other groups of images, due to the more complex image conditions, the differences in the images themselves make the D. J, P, and R curves changes significantly, and the average accuracy is slightly lower than that of the normal group.

From the overall goal, a lot of work needs to be perfected. First, due to the difficulty of data collection, the existing hazard warning algorithms are mainly trained and tested through public data sets, and the actual collected data needs to be used to further verify and optimize the algorithm; second, due to the limitation of research time, in medical In the imaging research, only the automatic extraction and 3D modeling of vascular intima contours were studied. The automatic identification of plaques and vulnerable plaques did not establish a mapping model between plaques and certain cardiovascular diseases in combination with clinical practice.

To guide clinical diagnosis and treatment, it can be used as the focus of the next research work; again, ECG signals and medical images can reflect the health of the heart and diagnose related cardiovascular diseases. But these two are signals of different technical levels. If the existing deep learning algorithm can be used to mine the internal relationship between the two and establish the correspondence between the two,

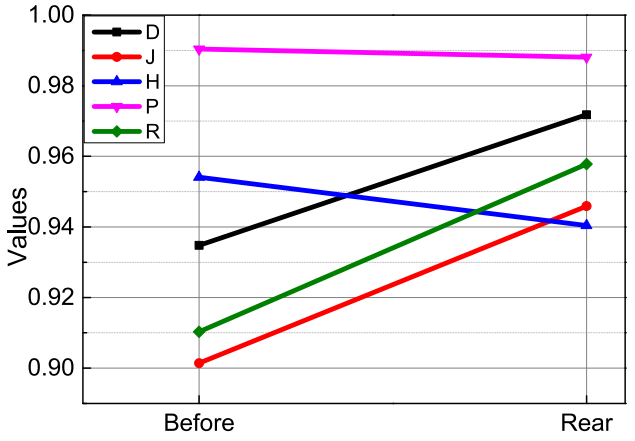

FIGURE 13. Average statistics of D, J, H, R and P before and after parameter optimization in sequence images.

the medical cost will be greatly reduced. Can be explored and verified in future research. Finally, if a fusion analysis model of ECG signals and medical images can be established for a certain type or type of cardiovascular disease, so that the two have complementary advantages and disadvantages, it will be very beneficial to the accurate diagnosis and early prevention of cardiovascular disease, and can be effective Reduce the mortality of cardiovascular disease. Restricted by the existing technical conditions, this work has not been carried out at present, and can be used as the next research work.

In order to more accurately evaluate the similarity between the algorithm and the gold standard model in this paper, we give the D, J, P and R change curves and their average statistics after the optimization of the algorithm and parameters in this paper. It can be seen that the algorithm of this paper can guarantee the accuracy of intima extraction in most cases, but in some cases, the automatically set parameters may prevent the algorithm from accurately positioning the boundary of the intima, and the parameters need to be revised. After the individual image parameters were revised, the large error points disappeared, and the established model is closer to the gold standard model as showed in Figure 13.

This paper mainly studies the intelligent analysis method of high-risk cardiovascular disease, makes full use of the portable and long-term acquisition characteristics of dynamic electrocardiogram, and studies the arrhythmia and SCD intelligent prediction algorithm on the level of the ECG signal. Constructed a sparse automatic coding deep neural network with a 4-layer stack structure to automatically extract the deep features of arrhythmia heartbeats, and realized the automatic recognition of 6 types of heartbeats through the surtax classifier. The in-depth feature can describe the input signal more accurately, and discuss and analyze the key parameters in the network. Taking full advantage of the ability of the echo state network to recognize time-domain signals, the accurate identification of sudden cardiac death signals was achieved by designing an ESN network with a multi-layer series structure. Using the signal 5 minutes before the occurrence of sudden death, accurate predictions were 93.04%, 95.36%, 94.20%, 94.20% and 94.78%. Taking full advantage of the high-precision and high-resolution characteristics of medical images, the linear label maximum flow algorithm is used to automatically extract the contour of the vascular intima in the coronary OCT image, for more accurate assessment of vascular stenosis and analysis of intravascular blood flow The academic characteristics provide a guarantee. According to the different tissue information contained in different OCT images, which have different gray distribution characteristics, the automatic selection method of gray label values based on the gray distribution characteristics of the image is studied to ensure the stability of the algorithm when extracting the inner film of different OCT images. And verify the effect of the algorithm under different interference of the inner membrane extraction. Make full use of the self-learning ability of the stack sparse automatic coding network for unlabeled data, and perform in-depth modeling and analysis of A-line in OCT images to achieve accurate identification of fibrosis, fibrosis-calcification, and fibrosis-lipid A-line, And based on the automatic generation algorithm of plaque area, the automatic extraction of plaque area was realized. On this basis, by analyzing the thickness of the fiber cap, the automatic identification of vulnerable plaques of thin fiber caps was realized.

IV. CONCLUSION

In this paper, CNN and LSTM deep learning models are proposed to classify and recognize serum electrolyte disorders. Determine the learning theory to dynamically model the ST-T segment in the ECG to obtain the serum electrolyte disorder. It reflects cardiac repolarization activity in three-dimensional space and more vividly the changes in electrical information under myocardial ischemia. In order to reveal the relationship between serum electrolyte disturbance and myocardial ischemia, this paper builds a neural network model to carry out end-to-end learning and training on serum electrolyte disturbance data to achieve positive or negative classification of myocardial ischemia, by testing serum electrolyte disturbance data collected in clinical experiments It shows that the model can achieve early detection of myocardial ischemia. To build a deep learning model to classify serum electrolyte disorders requires a lot of training data, but because a series of clinical trials has just begun, there is not much labeled data. Although data can be directly extracted through the hospital's information system, these data cannot be used immediately. Deep learning is currently superior to past methods in many fields, such as computer vision analysis, image classification and recognition, natural language processing, speech recognition and synthesis, and IoT sequence data classification, but there are still some problems that need further research, such as models Theoretical analysis, label-free data classification and model generalization ability and adaptive technology. In general, deep learning has opportunities and challenges in the field of medical disease diagnosis, and other methods need to be integrated to obtain higher accuracy. In addition, the

research object of this experiment is mainly concentrated in the population with high incidence of heart disease, such as inpatients, and it is not extended to the general population, resulting in more experimental data in the experimental data than negative medical data. With the continuous improvement of the data set, not only can the neural network model be further improved, but also the degree of serum electrolyte disturbance can be classified to achieve multi-classification to further verify the effect of electrocardiogram in the early detection of serum electrolyte disturbance.

REFERENCES

[1] C. D. Galloway, A. V. Valys, J. B. Shreibati, D. L. Treiman, F. L. Petterson, V. P. Gundotra, and D. E. Albert, "Development and validation of a deep-learning model to screen for hyperkalemia from the electrocardiogram," *JAMA Cardiol.*, vol. 4, no. 5, pp. 428–436, 2016.

[2] M. Sun, J. Baron, A. Dighe, P. Szolovits, R. G. Wunderink, T. Isakova, and Y. Luo, "Early prediction of acute kidney injury in critical care setting using clinical notes and structured multivariate physiological measurements," *Stud. Health Technol. Inform.*, vol. 264, pp. 368–372, Aug. 2019.

[3] S. Manaktala and S. R. Claypool, "Evaluating the impact of a computerized surveillance algorithm and decision support system on sepsis mortality," *J. Amer. Med. Inform. Assoc.*, vol. 24, no. 1, pp. 88–95, Jan. 2017.

[4] N. Khajehali and S. Alizadeh, "Extract critical factors affecting the length of hospital stay of pneumonia patient by data mining (case study: An iranian hospital)," *Artif. Intell. Med.*, vol. 83, pp. 2–13, Nov. 2017.

[5] P. F. Plouin, L. Amar, O. M. Dekkers, M. Fassnacht, A. P. Gimenez-Roqueplo, J. W. M. Lenders, C. Lussey-Lepoutre, and O. Steichen, "European society of endocrinology clinical practice guideline for long-term follow-up of patients operated on for a phaeochromocytoma or a paraganglioma," *Eur. J. Endocrinol.*, vol. 174, no. 5, pp. G1–G10, May 2016.

[6] M. R. Mathis, M. C. Engoren, H. Joo, M. D. Maile, K. D. Aaronson, M. L. Burns, and M. W. Sjoding, "Early detection of heart failure with reduced ejection fraction using perioperative data among noncardiac surgical patients: A machine-learning approach," *Anesthesia Analgesia*, vol. 130, no. 5, pp. 1188–1200, 2020.

[7] M. E. Hirschtritt, M. H. Bloch, and C. A. Mathews, "Obsessive-compulsive disorder: advances in diagnosis and treatment," *Jama*, vol. 317, no. 13, pp. 1358–1367, 2017.

[8] I. Solos and Y. Liang, "A historical evaluation of chinese tongue diagnosis in the treatment of septicemic plague in the pre-antibiotic era, and as a new direction for revolutionary clinical research applications," *J. Integrative Med.*, vol. 16, no. 3, pp. 141–146, May 2018.

[9] J. I. Wolfsdorf, N. Glaser, M. Agus, M. Fritsch, R. Hanas, A. Rewers, M. A. Sperling, and E. Codner, "ISPAD clinical practice consensus guidelines 2018: Diabetic ketoacidosis and the hyperglycemic hyperosmolar state," *Pediatric Diabetes*, vol. 19, pp. 155–177, Oct. 2018.

[10] T. J. Loftus, P. J. Tighe, A. C. Filiberto, P. A. Efron, S. C. Brakenridge, A. M. Mohr, P. Rashidi, G. R. Upchurch, and A. Bihorac, "Artificial intelligence and surgical decision-making," *Jama Surg.*, vol. 155, no. 2, pp. 148–158, 2020.

[11] M. Savarese, L. Maggi, A. Vihola, and P. H. Jonson, "Interpreting genetic variants in titin in patients with muscle disorders," *JAMA Neurol.*, vol. 75, no. 5, pp. 557–565, 2018.

[12] E. S. Rawson, P. M. Clarkson, and M. A. Tarnopolsky, "Perspectives on exertional rhabdomyolysis," *Sports Med.*, vol. 47, no. S1, pp. 33–49, Mar. 2017.

[13] S. Kanoria, F. P. Robertson, N. N. Mehta, G. Fusai, D. Sharma, and B. R. Davidson, "Effect of remote ischaemic preconditioning on liver injury in patients undergoing major hepatectomy for colorectal liver metastasis: A pilot randomised controlled feasibility trial," *World J. Surg.*, vol. 41, no. 5, pp. 1322–1330, May 2017.

[14] A. Brodeur, A. Wright, and Y. Cortes, "Hypothermia and targeted temperature management in cats and dogs," *J. Veterinary Emergency Crit. Care*, vol. 27, no. 2, pp. 151–163, Mar. 2017.

[15] P. Tiwari, K. L. Colborn, D. E. Smith, F. Xing, D. Ghosh, and M. A. Rosenberg, "Assessment of a machine learning model applied to harmonized electronic health record data for the prediction of incident atrial fibrillation," *JAMA Netw. Open*, vol. 3, no. 1, 2020, Art. no. e1919396.

[16] J. D. Koola, S. B. Ho, A. Cao, G. Chen, A. M. Perkins, S. E. Davis, and M. E. Matheny, "Predicting 30-day hospital readmission risk in a national cohort of patients with cirrhosis," *Digestive Diseases Sci.*, vol. 65, no. 4, pp. 1003–1031, Apr. 2020.

[17] M. S. Venäläinen, R. Klén, M. Mahmoudian, O. T. Raitakari, and L. L. Elo, "Easy-to-use tool for evaluating the elevated acute kidney injury risk against reduced cardiovascular disease risk during intensive blood pressure control," *J. Hypertension*, vol. 38, no. 3, pp. 511–518, Mar. 2020.

[18] R. R. Shah, "Anti-angiogenic tyrosine kinase inhibitors and reversible posterior leukoencephalopathy syndrome: Could hypomagnesaemia be the trigger?" *Drug Saf.*, vol. 40, no. 5, pp. 373–386, May 2017.

[19] M. R. Boylan, D. C. Perfetti, R. K. Elmallah, V. E. Krebs, C. B. Paulino, and M. A. Mont, "Does chronic corticosteroid use increase risks of readmission, thromboembolism, and revision after THA?" *Clin. Orthopaedics Rel. Res.*, vol. 474, no. 3, pp. 744–751, Mar. 2016.

[20] Y. Zhao, J. Le, L. Zhu, and M. Zuo, "Study on the effect of hypertensive treatment based on drug factor analysis model under the background of big data," *J. Intell. Fuzzy Syst.*, vol. 37, no. 3, pp. 3217–3230, Oct. 2019.

[21] M. Renaud, M. C. Moreira, B. B. Monga, D. Rodriguez, R. Debs, P. Charles, and M. Chaouch, "Clinical, biomarker, and molecular delineations and Genotype-Phenotype correlations of ataxia with oculomotor apraxia type 1," *JAMA Neurol.*, vol. 75, no. 4, pp. 495–502, 2018.

[22] M. J. London, G. G. Schwartz, K. Hur, and W. G. Henderson, "Association of perioperative statin use with mortality and morbidity after major noncardiac surgery," *JAMA Internal Med.*, vol. 177, no. 2, pp. 231–242, 2017.

[23] I. Hernández-Neuta, F. Neumann, J. Brightmeyer, T. B. Tis, N. Madaboosi, Q. Wei, A. Ozcan, and M. Nilsson, "Smartphone-based clinical diagnostics: Towards democratization of evidence-based health care," *J. internal Med.*, vol. 285, no. 1, pp. 19–39, 2019.

[24] C. Florkowski, A. Don-Wauchope, N. Gimenez, K. Rodriguez-Capote, J. Wils, and A. Zemlin, "Point-of-care testing (POCT) and evidence-based laboratory medicine (EBLM)–does it leverage any advantage in clinical decision making?" *Crit. Rev. Clin. Lab. Sci.*, vol. 54, nos. 7–8, pp. 471–494, 2017.

[25] A. Kumar, A. Deep, R. K. Gupta, V. Atam, and S. Mohindra, "Brain microstructural correlates of cognitive dysfunction in clinically and biochemically normal hepatitis c virus infection," *J. Clin. Experim. Hepatol.*, vol. 7, no. 3, pp. 198–204, Sep. 2017.

[26] D. H. Katz, R. C. Deo, F. G. Aguilar, S. Selvaraj, E. E. Martinez, L. Beussink-Nelson, K.-Y.-A. Kim, J. Peng, M. R. Irvin, H. Tiwari, D. C. Rao, D. K. Arnett, and S. J. Shah, "Phenomapping for the identification of hypertensive patients with the myocardial substrate for heart failure with preserved ejection fraction," *J. Cardiovascular Transl. Res.*, vol. 10, no. 3, pp. 275–284, Jun. 2017.

[27] N. Boy *et al.*, "Proposed recommendations for diagnosing and managing individuals with glutaric aciduria type I: Second revision," *J. Inherited Metabolic Disease*, vol. 40, no. 1, pp. 75–101, Jan. 2017.

[28] S. Montagnese, F. P. Russo, P. Amodio, P. Burra, A. Gasbarrini, C. Loguercio, G. Marchesini, M. Merli, F. R. Ponziani, O. Riggio, and C. Scarpignato, "Hepatic encephalopathy 2018: A clinical practice guideline by the italian association for the study of the liver (AISF)," *Digestive Liver Disease*, vol. 51, no. 2, pp. 190–205, Feb. 2019.

[29] L. M. Castello, M. Baldrighi, A. Panizza, E. Bartoli, and G. C. Avanzi, "Efficacy and safety of two different tolvaptan doses in the treatment of hyponatremia in the emergency department," *Internal Emergency Med.*, vol. 12, no. 7, pp. 993–1001, Oct. 2017.

[30] C. Eggers, F. G. Arendt, K. Hahn, I. W. Husstedt, M. Maschke, E. Neuen-Jacob, M. Obermann, T. Rosenkranz, E. Schielke, and E. Straube, "HIV-1-associated neurocognitive disorder: Epidemiology, pathogenesis, diagnosis, and treatment," *J. Neurol.*, vol. 264, no. 8, pp. 1715–1727, Aug. 2017.

[31] R. Raina, V. Krishnappa, T. Blaha, T. Kann, W. Hein, L. Burke, and A. Bagga, "Atypical hemolytic-uremic syndrome: An update on pathophysiology, diagnosis, and treatment," *Therapeutic Apheresis Dialysis*, vol. 23, no. 1, pp. 4–21, 2019.

[32] S. Nishi, Y. Ubara, Y. Utsunomiya, K. Okada, Y. Obata, H. Kai, H. Kiyomoto, S. Goto, T. Konta, Y. Sasatomi, Y. Sato, T. Nishino, K. Tsuruya, K. Furuichi, J. Hoshino, Y. Watanabe, K. Kimura, and S. Matsuo, "Evidence-based clinical practice guidelines for nephrotic syndrome 2014," *Clin. Experim. Nephrol.*, vol. 20, no. 3, pp. 342–370, Jun. 2016.

[33] C. Rhee, S. S. Kadri, J. P. Dekker, R. L. Danner, H.-C. Chen, D. Fram, F. Zhang, R. Wang, and M. Klompas, "Prevalence of antibiotic-resistant pathogens in culture-proven sepsis and outcomes associated with inadequate and broad-spectrum empiric antibiotic use," *JAMA Netw. Open*, vol. 3, no. 4, Apr. 2020, Art. no. e202899.

[34] K. Regev, B. C. Healy, F. Khalid, A. Paul, R. Chu, S. Tauhid, and S. Tummala, "Association between serum MicroRNAs and magnetic resonance imaging measures of multiple sclerosis severity," *JAMA Neurol.*, vol. 74, no. 3, pp. 275–285, 2017.

[35] A. V. Goules, T. P. Exarchos, V. C. Pezoulas, K. D. Kourou, A. I. Venetsanopoulou, S. De Vita, D. I. Fotiadis, and A. G. Tzioufas, "Sjögren's syndrome towards precision medicine: The challenge of harmonisation and integration of cohorts," *Clin. Exp. Rheumatol.*, vol. 37, no. 3, pp. 175–184, 2019.

[36] Y. Yeh, Y. Kuo, M. Huang, S. Hwang, J. Tsai, M. Kuo, and C. Chen, "Association of brain white matter lesions and atrophy with cognitive function in chronic kidney disease," *Int. J. Geriatric Psychiatry*, vol. 34, no. 12, pp. 1826–1832, Dec. 2019.

[37] P. S. Ustkoyuncu, A. S. Guven, H. G. Poyrazoglu, S. Gokay, F. Kardas, M. Kendirci, I. Gokcek, and Y. A. Torun, "Screening inherited metabolic disorder in children with intellectual disability and Epilepsy/Zeka Geriligi ve Epilepsisi Olan Cocuklarda Kalitsal Metabolik Hastalik Taramasi," *Turkish J. Neurol.*, vol. 25, no. 3, pp. 135–140, 2019.

[38] S. Jain, V. Ahuja, and J. K. Limdi, "Optimal management of acute severe ulcerative colitis," *Postgraduate Med. J.*, vol. 95, no. 1119, pp. 32–40, Jan. 2019.

[39] J. M. Bos, P. M. L. A. van den Bemt, W. Kievit, J. L. W. Pot, J. E. Nagtegaal, A. Wieringa, M. M. L. van der Westerlaken, G. J. van der Wilt, P. A. G. M. de Smet, and C. Kramers, "A multifaceted intervention to reduce drug-related complications in surgical patients," *Brit. J. Clin. Pharmacol.*, vol. 83, no. 3, pp. 664–677, 2017.

[40] C. McCudden, "The future of artificial intelligence and interpretative specialization in clinical biochemistry," *Clin. Biochem.*, vol. 50, no. 6, pp. 253–254, Apr. 2017.

[41] H. Ahmadi, M. Gholamzadeh, L. Shahmoradi, M. Nilashi, and P. Rashvand, "Diseases diagnosis using fuzzy logic methods: A systematic and meta-analysis review," *Comput. Methods Programs Biomed.*, vol. 161, pp. 145–172, Jul. 2018.

[42] A. T. N. Tita, J. M. Szychowski, K. Boggess, G. Saade, S. Longo, E. Clark, S. Esplin, K. Cleary, R. Wapner, K. Letson, M. Owens, A. Abramovici, N. Ambalavanan, G. Cutter, and W. Andrews, "Adjunctive azithromycin prophylaxis for cesarean delivery," *New England J. Med.*, vol. 375, no. 13, pp. 1231–1241, Sep. 2016.

[43] K. Everaert, F. Hervé, R. Bosch, R. Dmochowski, M. Drake, H. Hashim, C. Chapple, P. Van Kerrebroeck, S. Mourad, P. Abrams, and A. Wein, "International continence society consensus on the diagnosis and treatment of nocturia," *Neurourol. Urodyn.*, vol. 38, no. 2, pp. 478–498, Feb. 2019.

[44] A. Thorell, A. D. MacCormick, S. Awad, N. Reynolds, D. Roulin, N. Demartines, M. Vignaud, A. Alvarez, P. M. Singh, and D. N. Lobo, "Guidelines for perioperative care in bariatric surgery: Enhanced recovery after surgery (ERAS) society recommendations," *World J. Surg.*, vol. 40, no. 9, pp. 2065–2083, Sep. 2016.

[45] M. Li, E. P. Diamandis, D. Grenache, and M. J. Joyner, "Direct-to-consumer testing," *Clin. Chem.*, vol. 63, no. 3, pp. 635–641, 2017.

[46] B. Knier, G. Leppenetier, C. Wetzlmair, and L. Aly, "Association of retinal architecture, intrathecal immunity, and clinical course in multiple sclerosis," *JAMA Neurol.*, vol. 74, no. 7, pp. 847–856, 2017.

[47] M. S. Fejzo, J. Trovik, I. J. Grooten, K. Sridharan, T. J. Roseboom, Å. Vikanes, R. C. Painter, and P. M. Mullin, "Nausea and vomiting of pregnancy and hyperemesis gravidarum," *Nature Rev. Disease Primers*, vol. 5, no. 1, p. 26, 2019.

[48] A. L. Zaenglein *et al.*, "Guidelines of care for the management of acne vulgaris," *J. Amer. Acad. Dermatol.*, vol. 74, no. 5, pp. 945–973, 2016.

[49] A. McKeon, "Autoimmune encephalopathies and dementias," *CONTINUUM, Lifelong Learn. Neurol.*, vol. 22, no. 2, pp. 538–558, Apr. 2016.

[50] Y. Yildiz, E. Pektas, A. Tokatli, and G. Haliloglu, "Hereditary dopamine transporter deficiency syndrome: Challenges in diagnosis and treatment," *Neuropediatrics*, vol. 48, no. 1, pp. 049–052, 2017.

[51] K. Xia, X. Gu, and Y. Zhang, "Oriented grouping-constrained spectral clustering for medical imaging segmentation," *Multimedia Syst.*, vol. 26, no. 1, pp. 27–36, Feb. 2020.

[52] K. Xia, H. Yin, P. Qian, Y. Jiang, and S. Wang, "Liver semantic segmentation algorithm based on improved deep adversarial networks in combination of weighted loss function on abdominal CT images," *IEEE Access*, vol. 7, pp. 96349–96358, 2019.

[53] S. H. Wang, Y. Zhang, Y. J. Li, W. J. Jia, F. Y. Liu, M.-M. Yang, and Y.-D. Zhang, "Single slice based detection for Alzheimer's disease via wavelet entropy and multilayer perceptron trained by biogeography-based optimization," *Multimedia Tools Appl.*, vol. 77, no. 9, pp. 10393–10417, 2018.

[54] S. Wang, J. Sun, I. Mehmood, C. Pan, Y. Chen, and Y.-D. Zhang, "Cerebral micro-bleeding identification based on a nine-layer convolutional neural network with stochastic pooling," *Concurrency Comput., Pract. Exper.*, vol. 32, no. 1, p. e5130, 2020.

[55] Y.-D. Zhang, V. V. Govindaraj, C. Tang, W. Zhu, and J. Sun, "High performance multiple sclerosis classification by data augmentation and AlexNet transfer learning model," *J. Med. Imag. Health Informat.*, vol. 9, no. 9, pp. 2012–2021, Dec. 2019.

[56] Y. Zhang, S. Wang, Y. Sui, M. Yang, and B. Liu, "Multivariate approach for Alzheimer's disease detection using stationary wavelet entropy and predator-prey particle swarm optimization," *J. Alzheimer's Disease*, vol. 65, no. 3, pp. 855–869, 2018.

[57] C. Kang, X. Yu, S.-H. Wang, D. Guttery, H. Pandey, Y. Tian, and Y. Zhang, "A heuristic neural network structure relying on fuzzy logic for images scoring," *IEEE Trans. Fuzzy Syst.*, early access, Jan. 13, 2020, doi: 10.1109/TFUZZ.2020.2966163.

[58] S.-H. Wang, Y.-D. Zhang, M. Yang, B. Liu, J. Ramirez, and J. M. Gorriz, "Unilateral sensorineural hearing loss identification based on double-density dual-tree complex wavelet transform and multinomial logistic regression," *Integr. Comput.-Aided Eng.*, vol. 26, no. 4, pp. 411–426, Sep. 2019.

[59] S.-H. Wang, J. Sun, P. Phillips, G. Zhao, and Y.-D. Zhang, "Polarimetric synthetic aperture radar image segmentation by convolutional neural network using graphical processing units," *J. Real-Time Image Process.*, vol. 15, no. 3, pp. 631–642, Oct. 2018.

[60] S. Wang, C. Tang, J. Sun, Y. Zhang, "Cerebral micro-bleeding detection based on densely connected neural network," *Frontiers Neurosci.*, vol. 13, p. 422, Feb. 2019.

[61] S.-H. Wang, S. Xie, X. Chen, D. S. Guttery, C. Tang, J. Sun, and Y.-D. Zhang, "Alcoholism identification based on an AlexNet transfer learning model," *Frontiers Psychiatry*, vol. 10, Apr. 2019.

[62] Y. Jiang, Z. Deng, F.-L. Chung, G. Wang, P. Qian, K.-S. Choi, and S. Wang, "Recognition of epileptic EEG signals using a novel multiview TSK fuzzy system," *IEEE Trans. Fuzzy Syst.*, vol. 25, no. 1, pp. 3–20, Feb. 2017.

[63] Y. Jiang, F.-L. Chung, S. Wang, Z. Deng, J. Wang, and P. Qian, "Collaborative fuzzy clustering from multiple weighted views," *IEEE Trans. Cybern.*, vol. 45, no. 4, pp. 688–701, Apr. 2015.

JIAN WANG graduated from the Fujian Medical University of Clinical Medicine, in 1997. He studied at the Department of Endocrinology and Metabolism, Fujian Institute of Endocrinology, Fujian Medical University Union Hospital. His research interests include thyroid disease and electrolyte imbalance.

YAN PING WANG graduated from the Fujian Medical University of Clinical Medicine, in 2007. She studied at the Department of Endocrinology and Metabolism, Fujian Institute of Endocrinology, Fujian Medical University Union Hospital. Her research interests include diabetes and osteoporosis.

YAO CHEN graduated from the Fujian Medical University of Clinical Medicine, in 1985. She studied at the Department of Endocrinology and Metabolism, Fujian Institute of Endocrinology, Fujian Medical University Union Hospital. Her research interests include diabetes and thyroid disease.

PEIJI HUANG graduated from the Fujian Medical University of Clinical Medicine, in 1985. He studied at the Department of Endocrinology and Metabolism, Fujian Institute of Endocrinology, Fujian Medical University Union Hospital. His research interests include diabetes and osteoporosis.